Expanded View Figures

Figure EV1. Expression of IL-38 in different tissues and the expression of IL-1 family members in cSCC and DMBA/TPA-induced mouse tumors.

A IL-38 expression in various tissues sourced from control subjects (n = 6–860) using the GTEx database.
B Representative immunohistochemical staining micrographs of IL-38 and rabbit IgG in human normal skin. Scale bars represent 200 μm.
C Relative expression of IL-1 family members in human normal tissues (n = 9) and cSCC (n = 18) were analyzed using Geo Datasets (GSE98767).
D Relative expression of IL-1 family members in normal tissues (n = 9) and cSCC (n = 38) of mice analyzed using Geo Datasets (GSE63967).
E Representative micrographs of human skin sections stained with anti-IL-18 antibody from normal patients (n = 11) and tumors of cSCC patients (n = 13). Scale bars represent 100 μm. The graph shows the quantification of mean IL-18 expression per high-powered field in tissues.
F The dorsal hair of normal C57/BL6 mice was shaved and treated with DMBA/TPA twice a week for 32 weeks to induce skin tumors. Representative micrographs of mouse normal skin (n = 6) and tumor (n = 6) sections stained with anti-IL-18 antibody. Scale bars represent 100 μm. The graph shows the quantification of mean IL-38 expression in tissues.
G Representative western blot bands indicating IL-18 in mouse normal skin (n = 3) and DMBA/TPA-induced tumors (n = 3). The graph shows the quantification of mean IL-18 expression in tissues. β-actin blots of Figs EV1G and EV3F are derived from the same experiment.

Data information: Error bars represent the mean ± SD. All data are biological replicates. ns, not significant; *P < 0.05; **P < 0.01; ***P < 0.001; P values were calculated using Student's t-test.

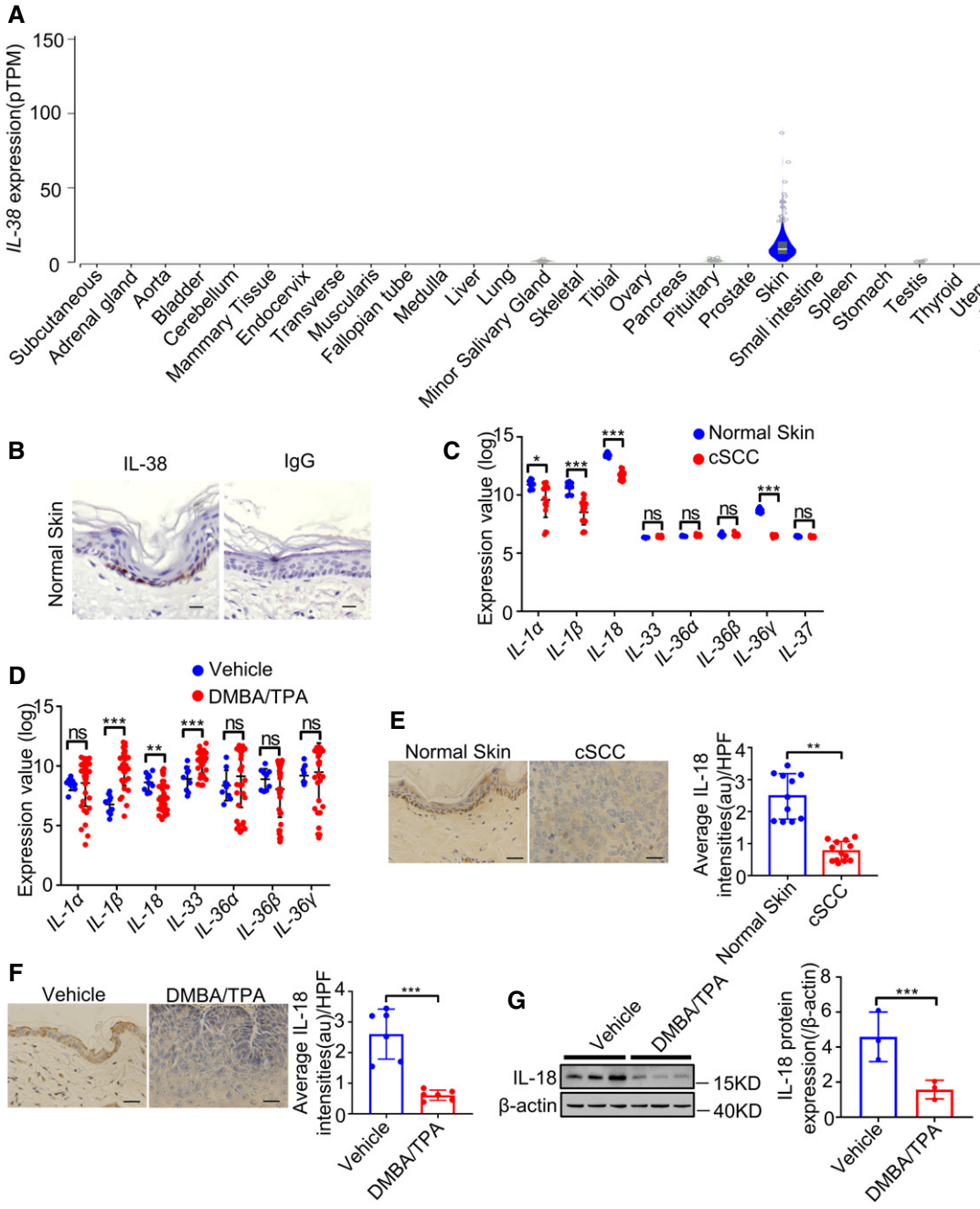
A
IL-38 expression(pTPM)
150
100
50
0
Subcutaneous
Adrenal gland
Aorta
Bladder
Cerebellum
Mammary Tissue
Endocervix
Transverse
Muscularis
Fallopian tube
Medulla
Liver
Lung
Minor Salivary Gland
Skeletal
Tibial
Ovary
Pancreas
Pituitary
Prostate
Skin
Small intestine
Spleen
Stomach
Testis
Thyroid
Uterus
Vagina
Whole Blood
B
IL-38
IgG
Normal Skin
C
Normal Skin
cSCC
Expression value (log)
IL-1α
IL-1β
IL-18
IL-33
IL-36α
IL-36β
IL-36γ
IL-37
D
Vehicle
DMBA/TPA
Expression value (log)
E
Normal Skin
cSCC
Average IL-18 intensities(au)/HPF
F
Vehicle
DMBA/TPA
Average IL-18 intensities(au)/HPF
G
Vehicle
DMBA/TPA
IL-18
β-actin
15KD
40KD
IL-18 protein expression(/β-actin)

Figure EV1.

Figure EV2. Construction and identification of keratinocytes IL-38-specific knockout mice and effect of keratinocyte-specific IL-38 deficiency on epidermal barrier.

A Construction of *Il-38*-loxP (*Il-38*$^{f/f}$) mice.
B Typical genetic cross scheme of keratinocyte IL-38-specific knockout (*K14*$^{Cre/+}$-*Il-38*$^{f/f}$) mice.
C PCR analysis of WT mice (at 317 and 245 bp) and *Il-38*-loxP mice (at 387 and 373 bp).
D PCR analysis of keratin 14 promoter directing expression of Cre recombinase(left) and deletion of IL-38 (right).
E Relative expression of *IL-38* in the epidermal splits of *Il-38*$^{f/f}$ (n = 4) and *K14*$^{Cre/+}$-*Il-38*$^{f/f}$ (n = 4) mice.
F Representative western blot bands indicating IL-38 in the epidermal splits of *Il-38*$^{f/f}$ and *K14*$^{Cre/+}$-*Il-38*$^{f/f}$ mice.
G Appearance of *Il-38*$^{f/f}$ and *K14*$^{Cre/+}$-*Il-38*$^{f/f}$ mice.
H Cumulative body weight changes in *Il-38*$^{f/f}$ (n = 12) and *K14*$^{Cre/+}$-*Il-38*$^{f/f}$ (n = 12) mice in 60 days.
I Representative histological photographs of skin stained with hematoxylin-eosin (H&E) from *Il-38*$^{f/f}$ (n = 5) and *K14*$^{Cre/+}$-*Il-38*$^{f/f}$ (n = 5) mice. Scale bars represent 100 μm. The graph shows the quantification of epidermal thickness.
J Skin barrier-dependent dye exclusion assay using toluidine blue in *Il-38*$^{f/f}$ mice (n = 5) and *K14*$^{Cre/+}$-*Il-38*$^{f/f}$ littermate (n = 5) at birth.
K TEWL assay measured on ventral surface of newborn *Il-38*$^{f/f}$ mice (n = 6) and *K14*$^{Cre/+}$-*Il-38*$^{f/f}$ littermate (n = 6).
L Representative micrographs of cornified cell envelopes from *Il-38*$^{f/f}$ (n = 4) and *K14*$^{Cre/+}$-*Il-38*$^{f/f}$ (n = 4) mice. Scale bars represent 100 μm. The graph shows the number of cornified cell envelopes per square millimeter.
M Representative immunohistochemical staining micrographs of CD45 in the skin of *Il-38*$^{f/f}$ (n = 5) and *K14*$^{Cre/+}$-*Il-38*$^{f/f}$ (n = 5) mice. Scale bars represent 100 μm. The graph shows average intensities of CD45 per high-powered field.

Data information: Error bars represent the mean ± SD. All data are biological replicates. ns, not significant; *P < 0.05; **P < 0.01; ***P < 0.001; P values were calculated using Student's t-test.

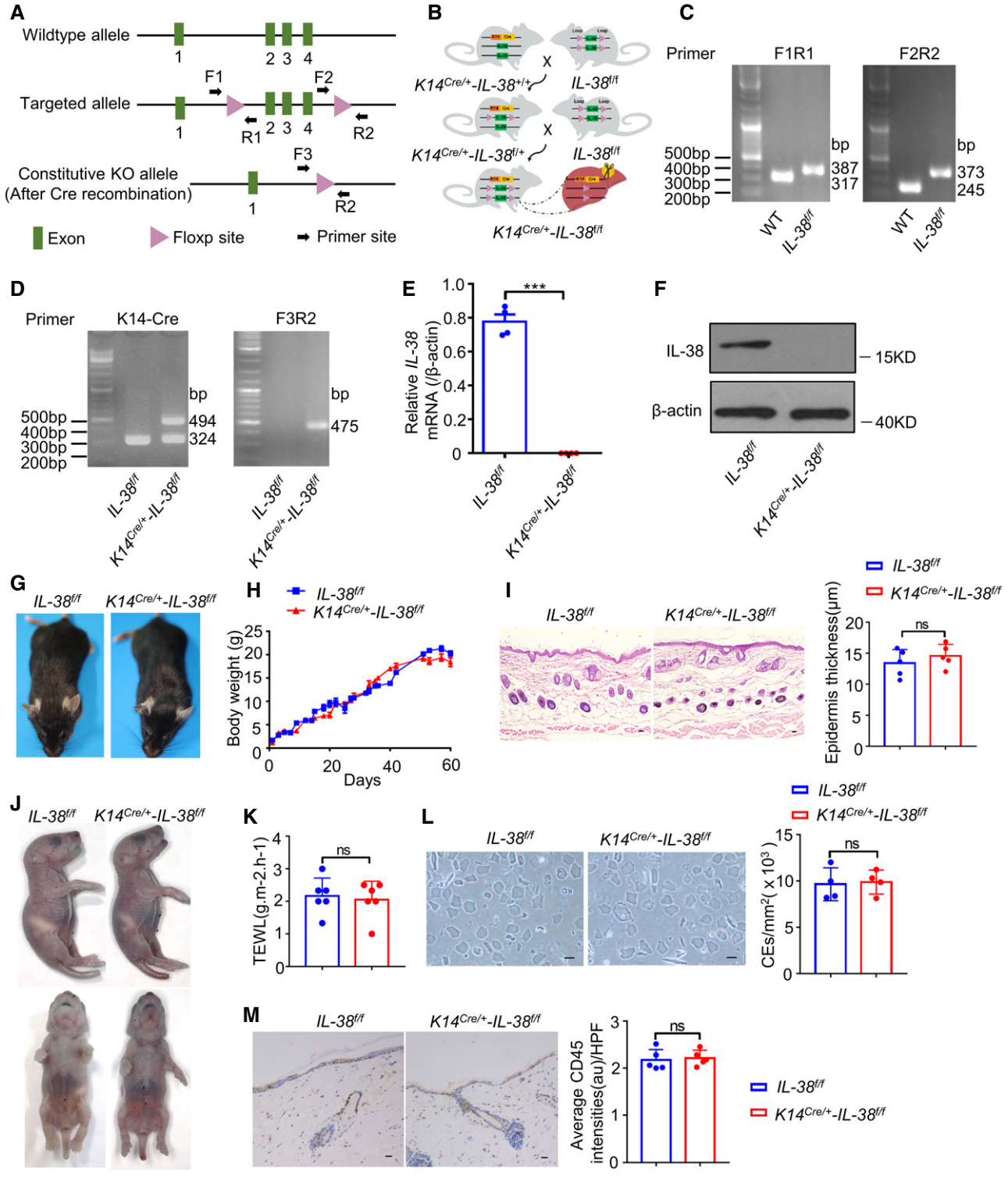
A
Wildtype allele
Targeted allele
Constitutive KO allele
(After Cre recombination)
Exon
Floxp site
Primer site
B
C
Primer
F1R1
F2R2
500bp
400bp
300bp
200bp
387
317
373
245
WT
IL-38f/f
D
Primer
K14-Cre
F3R2
494
324
475
E
Relative IL-38 mRNA (/β-actin)
***
F
IL-38
β-actin
15KD
40KD
G
H
Body weight (g)
Days
I
Epidermis thickness(μm)
ns
J
K
TEWL(g.m-2.h-1)
L
CEs/mm2(×10³)
M
Average CD45 intensities(au)/HPF

Figure EV2.

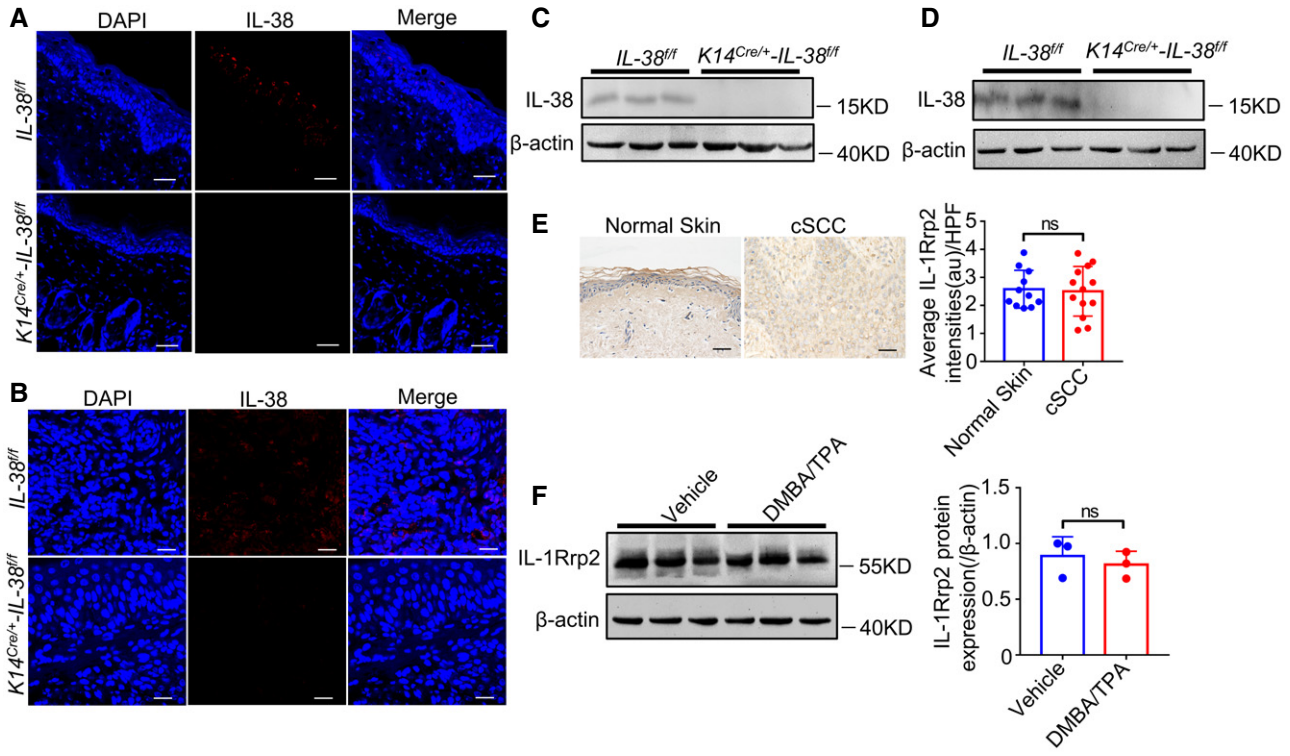

Figure EV3. Expression of IL-38 and IL-1Rrp2 in tissues.

A–D The dorsal hair of normal C57/BL6 mice was shaved and treated with DMBA/TPA twice a week for 3 weeks to induce the skin inflammation (A and C). (A) Representative immunofluorescent staining micrographs of IL-38 in the skin of *Il-38*$^{f/f}$ and *K14*$^{Cre/+}$-*Il-38*$^{f/f}$ mice. Scale bars represent 100 μm. (C) Relative expression of IL-38 in the skin of *Il-38*$^{f/f}$ (n = 3) and *K14*$^{Cre/+}$-*Il-38*$^{f/f}$ (n = 3) mice was detected by western blot. The dorsal hair of normal C57/BL6 mice was shaved and treated with DMBA/TPA twice a week for 32 weeks to induce the skin tumors (B and D). (B) Representative immunofluorescent staining micrographs of IL-38 in the tumors of *Il-38*$^{f/f}$ and *K14*$^{Cre/+}$-*Il-38*$^{f/f}$ mice. Scale bars represent 100 μm. (D) Relative expression of IL-38 in the tumors of *Il-38*$^{f/f}$ (n = 3) and *K14*$^{Cre/+}$-*Il-38*$^{f/f}$ (n = 3) mice was detected by western blot.

E Representative immunohistochemical staining micrographs of IL-1Rrp2 from normal patients (n = 11) and tumors of cSCC patients (n = 13). Scale bars represent 100 μm. The graph shows average intensities of IL-1Rrp2 per high-powered field in tissues.

F Relative expression of IL-1Rrp2 in mouse normal skin (n = 3) and DMBA/TPA-induced tumors (n = 3). The graph shows the quantification of mean IL-1Rrp2 expression in tissues.

Data information: Error bars represent the mean ± SD. All data are biological replicates. ns, not significant; P values were calculated using Student's t-test.

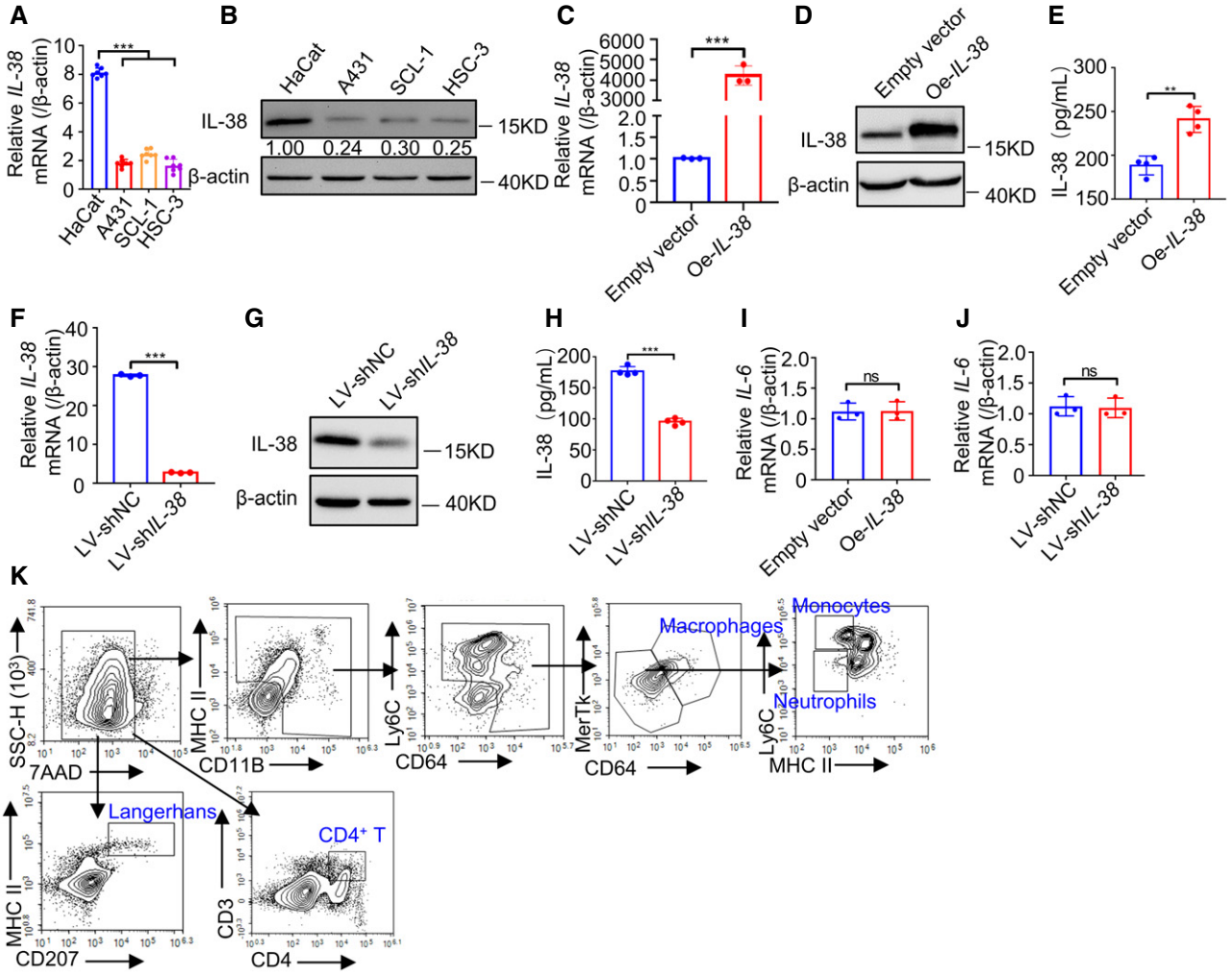

Figure EV4. Expression of IL-38 and IL-6 in SCC cell lines and the gating strategy for flow cytometry.

A Relative expression of *IL-38* in normal skin cells ($n = 7$) and SCC cells ($n = 7$) determined using qPCR.

B Relative expression levels of IL-38 in normal skin and SCC cells were detected using western blot.

C–E The *IL-38* overexpression cell line was constructed by transfecting A431 cells with the pcDNA3.1-*IL-38* vector expressing IL-38 and pcDNA3.1 empty vector. (C) Relative expression of *IL-38* was determined using qPCR. (D) Relative expression of IL-38 was detected using western blotting. (E) The secretion of IL-38 was measured using ELISA.

F–H Lentiviruses containing IL-38 shRNA or Negative Control shRNA were used to infect A431 cells. (F) Relative expression of *IL-38* was determined using qPCR. (G) Relative expression of IL-38 was detected using western blot. (H) IL-38 secretion was measured using ELISA.

I Relative expression of *IL-6* in *IL-38*-overexpressed A431 cells ($n = 3$) was determined using qPCR.

J Relative expression of *IL-6* in *IL-38*-knockdown A431 cells ($n = 3$) was determined using qPCR.

K The flow cytometry gating strategy for immune cell detection in DMBA/TPA-treated skin.

Data information: Error bars represent the mean ± SD. All data are biological replicates. ns, not significant; $*P < 0.05$; $**P < 0.01$; $***P < 0.001$; *P* values were calculated using one-way ANOVA (A) or Student's *t*-test (C, E, F, and H-J).

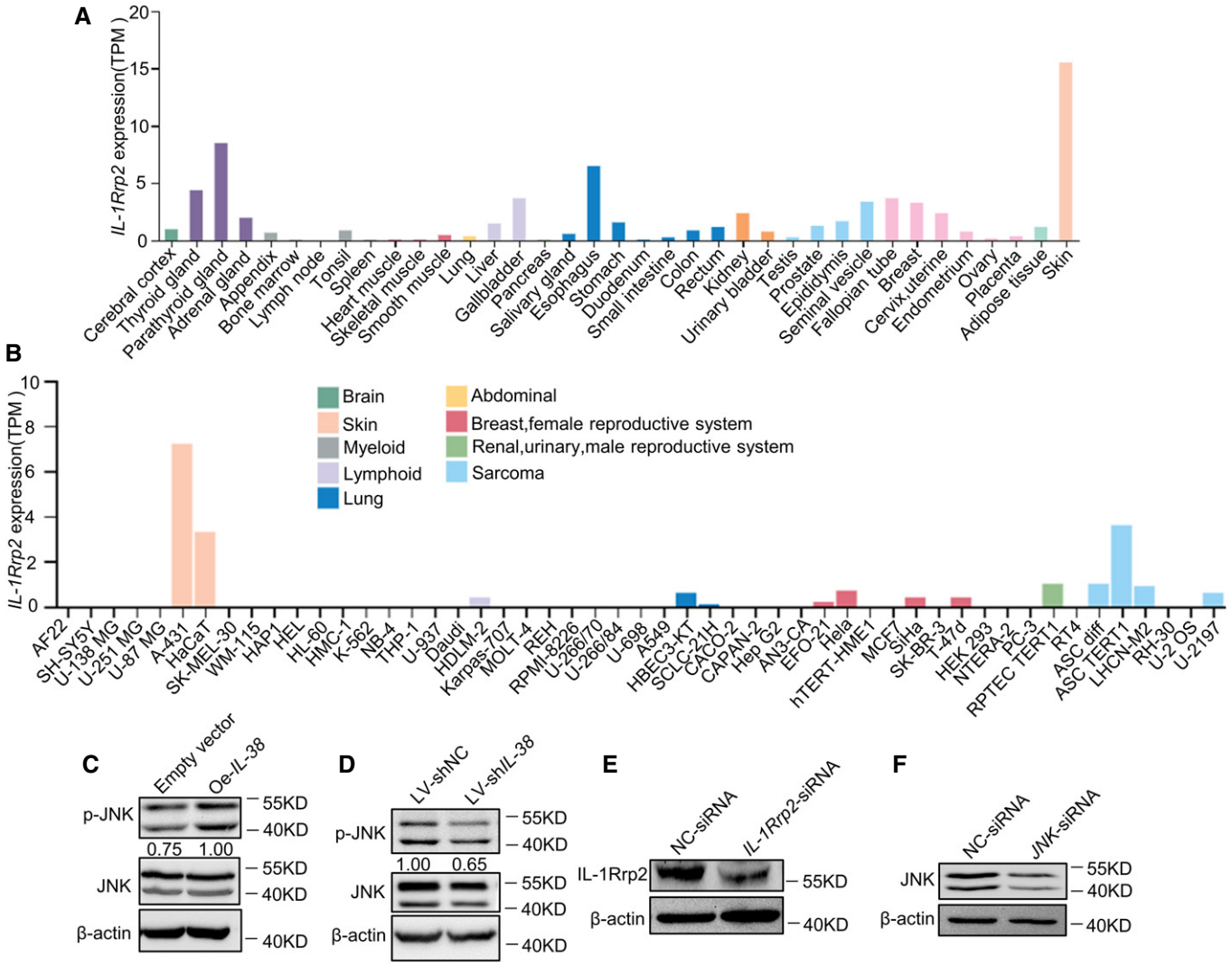

Figure EV5. Expression of IL-1Rrp2 in tissues and cell lines and the effect of IL-38 on JNK activation in A431 cell line.

A, B Relative expression of *IL-1Rrp2* in human normal tissues (A) or cell lines (B) based on TPM values. Data were obtained from the Human Protein Atlas Dataset available from proteinatlas.org.

C Cell extracts prepared from A431 cells transfected with a mock mammalian expression vector (left) or an expression vector encoding IL-38 (right), were blotted with anti-phospho-JNK, anti-JNK, or anti-β-actin antibodies.

D Cell extracts prepared from A431 cells infected with lentiviruses containing Negative Control shRNA (left) or *IL-38* shRNA (right) were probed using anti-phospho-JNK, anti-JNK, or anti-β-actin antibodies.

E The expression of IL-1Rrp2 in A431 cells transfected with *IL-1Rrp2*-siRNA was detected using western blot.

F The expression of JNK in A431 cells transfected with *JNK*-siRNA was detected using western blot.